
Early Stopping without a Validation Set

Maren Mahsereci¹ Lukas Balles¹ Christoph Lassner^{2,1} Philipp Hennig¹

Abstract

Early stopping is a widely used technique to prevent poor generalization performance when training an over-expressive model by means of gradient-based optimization. To find a good point to halt the optimizer, a common practice is to split the dataset into a training and a smaller validation set to obtain an ongoing estimate of the generalization performance. In this paper we propose a novel early stopping criterion which is based on fast-to-compute, local statistics of the computed gradients and entirely removes the need for a held-out validation set. Our experiments show that this is a viable approach in the setting of least-squares and logistic regression as well as neural networks.

1. Introduction

The training of parametric machine learning models usually involves minimizing an expected loss (risk) of the form

$$\mathcal{L}(w) = \mathbf{E}_{x \sim p(x)} [\ell(w, x)], \quad (1)$$

where the loss function $\ell(w, x)$ quantifies the performance of parameter vector $w \in \mathbb{R}^D$ on data point x . In practice though, the data distribution $p(x)$ is usually unknown, and instead the *empirical risk* is optimized which approximates Eq. 1:

$$L_{\mathcal{D}}(w) = \frac{1}{M} \sum_{x \in \mathcal{D}} \ell(w, x). \quad (2)$$

Here \mathcal{D} denotes a dataset of size $M = |\mathcal{D}|$ with instances drawn independently from $p(x)$. Often there is easy access to the gradient of ℓ and gradient-based optimizers can be used to minimize the empirical risk. The gradient descent (GD) algorithm for example updates an estimate w_t for the minimizer of $L_{\mathcal{D}}$ according to $w_{t+1} = w_t - \alpha_t \nabla L_{\mathcal{D}}(w_t)$ with

$$\nabla L_{\mathcal{D}}(w) = \frac{1}{M} \sum_{x \in \mathcal{D}} \nabla \ell(w, x) \quad (3)$$

and some hand-tuned or adaptive step sizes α_t . In practice, however, evaluating $\nabla L_{\mathcal{D}}$ can become expensive for very large M thus making it impossible to make progress in a reasonable time. Instead, stochastic optimization methods are used, which use coarser but much cheaper gradient estimates by randomly choosing a mini-batch $\mathcal{B} \subset \mathcal{D}$ of size $|\mathcal{B}| = m \ll M$ from the training set and computing

$$\nabla L_{\mathcal{B}}(w) = \frac{1}{m} \sum_{x \in \mathcal{B}} \nabla \ell(w, x). \quad (4)$$

The gradient descent update then becomes $w_{t+1} = w_t - \alpha_t \nabla L_{\mathcal{B}}(w_t)$ and the corresponding iterative algorithm is commonly known as stochastic gradient descent (SGD).

1.1. Overfitting, Regularization and Early-Stopping

Since the risk \mathcal{L} is virtually always unknown, a key question arising when minimizing the empirical risk $L_{\mathcal{D}}$ is how the performance of a model trained on a finite dataset \mathcal{D} generalizes to unseen data. Performance can be measured by the loss itself or other quantities, e.g., the mean accuracy in classification problems. Typically, to measure the generalization performance a finite *test set* is entirely withheld from the training procedure and the performance of the final model is evaluated on it. This test loss, however, is also only an estimator for \mathcal{L} (in the same sense as the train loss) with finite precision and drops in accuracy with decreasing test set size.

If the used model is overly expressive, minimizing the empirical risk (Eq. 2) exactly – or close to exactly – will usually result in poor test performance, since the model overfits to the training data. There is a range of measures that can be taken to mitigate this effect; classic textbooks like Bishop (2006) give a neat overview over general concepts, chapter 7 of Goodfellow et al. (2016) gives a comprehensive summary targeted at deep learning. Some widely used concepts are briefly discussed in the following paragraphs.

Model selection techniques choose a model among a hypothesis class which, under some measure, has the closest level of complexity to the given dataset. This directly alters the form of the loss function ℓ in Eq. 2 and algorithmically performs an outer optimization (first find a good ℓ , then optimize $L_{\mathcal{D}}$), such that the final optimization on $L_{\mathcal{D}}$ is performed on an adequately expressive model. This can –

¹Max Planck Institute for Intelligent Systems, Spemannstraße, Tübingen, Germany ²Bernstein Center for Computational Neuroscience, Otfried-Müller-Str. 25, Tübingen, Germany. Correspondence to: Maren Mahsereci <mmahsereci@tue.mpg.de>.

but does not need to – constrain the number of variables of the model. In the case of deep neural networks the number of variables can even significantly exceed the number of training examples (Krizhevsky et al., 2012; Simonyan & Zisserman, 2014; Szegedy et al., 2015; He et al., 2016).

If the dataset is not sufficiently representative of the data distribution, an opposite (but not excluding the above) approach is to artificially enhance its expressiveness to match a complex model. *Data augmentation* techniques try to artificially enlarge the training set by adding transformations/perturbations of the training data. This can range from injecting noise (Sietsma & Dow, 1991; Vincent et al., 2008) to carefully tuned contrast and colorspace augmentation (Krizhevsky et al., 2012).

Finally, a widely-used provision against overfitting is to add regularization terms to the objective function that penalize the parameter vector w , typically measured by the L_1 or L_2 norm (Krogh & Hertz, 1991). These terms constrain the magnitude of w and tend to drive individual parameters to zero, enforcing sparsity (especially when using L_1 norm) (Bishop, 2006; Goodfellow et al., 2016). In the linear case, the LASSO method (Tibshirani, 1996) is a well-known and widely used strategy for regularization.

Despite these countermeasures, high-capacity models will often overfit in the course of the optimization process. While the loss on the training set decreases throughout the optimization procedure, the test loss saturates at some point and starts to increase again. This undesirable effect is usually countered by *early stopping* the optimization process, meaning that for a *given* model the optimizer is halted, if a user-designed early stopping criterion is met. This is complementary to the model and data design techniques mentioned above and does not undo eventual poor design choices of ℓ . It merely ensures that we do not minimize the empirical risk $L_{\mathcal{D}}$ of a given model beyond the point of best generalization. In practice, however, it is often more accessible to ‘early-stop’ a high-capacity model for algorithmic purposes or because of restrictions to a specific model class and thus preferred or even enforced by the model designer.

A well-known early stopping criterion utilizes the loss of a *validation set* (Morgan & Bourlard, 1989; Reed, 1993; Prechelt, 2012) For this, a (usually small) portion of the training data is split off and its loss is used as an estimate of the generalization loss \mathcal{L} (again in the same sense as Eq. 2), leaving less effective training data to define the training loss $L_{\mathcal{D}}$. An ongoing estimate of this generalization performance is then tracked and the optimizer is halted when the generalization performance drops again. This procedure has many advantages, especially for very large datasets where splitting off a part has minor or no effect on the generalization performance of the learned model. Nevertheless, there are a few obvious drawbacks. Evaluating

the model on the validation set in regular intervals can be computationally expensive. More importantly, the choice of the *size* of the validation set poses a highly intricate trade-off. The performance measured on the validation set is only an imperfect estimate of the generalization performance. A small validation set results in low-precision estimates of the generalization performance, which can lead to a misguided stopping decision. A large validation set yields reliable estimates of the generalization performance, but reduces the effective amount of training data, depriving the model of potentially valuable information. This trade-off is not easily resolved, since it is influenced by properties of the data distribution (the variance Λ introduced in Eq. (5) below) and subject to practical considerations, e.g., redundancy in the dataset.

Recently Maclaurin et al. (2015) motivated an early-stopping criterion based on the interpretation of (stochastic) gradient descent in the framework of variational inference. It is based on estimating the marginal likelihood by tracking the change in entropy of the posterior distribution of w , which is induced by each optimization step. It remains unclear however if this approach is viable in practice.

The following section motivates and derives a cheap and scalable early stopping criterion which is solely based on local statistics of the computed gradients. In particular, it does not require a held-out validation set, thus enabling the optimizer to use *all* available training data.

2. Model

In this section, a novel criterion for early stopping is derived. Section 2.1 introduces notation and basic model assumptions, Section 2.2 motivates the idea behind an evidence based early stopping criterion and builds intuition. Section 2.3 first deals with the more intuitive case of gradient descent and derives a stopping criterion for it and Section 2.4 introduces a straightforward extension for stochastic gradient descent.

2.1. Distribution of Gradient Estimators

Let \mathcal{S} be some set of instances sampled independently from $p(x)$. The following holds for any \mathcal{S} , but specifically for the training set \mathcal{D} or a subsampled mini-batch \mathcal{B} and any validation or test set. Using the same notation as in Equations 2 and 3, $L_{\mathcal{S}}(w)$ and $\nabla L_{\mathcal{S}}(w)$ are unbiased estimators of $\mathcal{L}(w)$ and $\nabla \mathcal{L}(w)$ respectively. Since the elements in \mathcal{S} are independent draws from $p(x)$, by the Central Limit Theorem $L_{\mathcal{S}}(w)$ and $\nabla L_{\mathcal{S}}(w)$ are approximately normal

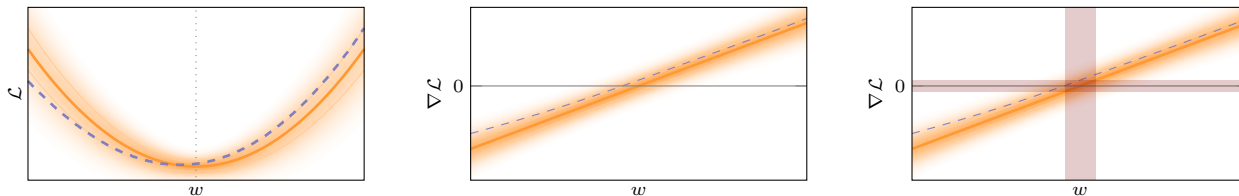


Figure 1. Sketch of early stopping criterion. **Left:** marginal distribution of function values defined by first line of Eq. 5. Mean \mathcal{L} in thick solid orange, ± 1 standard deviations in light orange. Pdf as shaded orange. The *full* dataset defines *one* realization which is shown in dashed blue (same as L_M of Eq. 2). **Middle:** same as left plot but for marginal of gradients. The pdf is defined by the second line in Eq. 5 and the corresponding ∇L_M (Eq. 3) is shown in dashed blue. **Right:** orange and blue same as middle plot. The vertical red shaded area shows the region of ± 1 standard deviation of possible minima (where ∇L_M is likely to be zero). If gradients are within this area, the optimization process is halted. This can be translated into a simple stopping criterion (horizontal shaded area, text for details). Again, if gradients are within this area, the optimizer stops.

distributed according to

$$\begin{aligned} L_S(w) &\sim \mathcal{N}\left(\mathcal{L}(w), \frac{\Lambda(w)}{|\mathcal{S}|}\right), \\ \nabla L_S(w) &\sim \mathcal{N}\left(\nabla \mathcal{L}(w), \frac{\Sigma(w)}{|\mathcal{S}|}\right) \end{aligned} \quad (5)$$

with population (co-)variances $\Lambda(w)$ and $\Sigma(w)$ of function value and gradients respectively

$$\begin{aligned} \Lambda(w) &= \mathbf{var}_{x \sim p(x)}[\ell(w, x)] \in \mathbb{R} \\ \Sigma(w) &= \mathbf{cov}_{x \sim p(x)}[\nabla \ell(w, x)] \in \mathbb{R}^{D \times D}. \end{aligned} \quad (6)$$

The (co-)variances of $L_S(w)$ and $\nabla L_S(w)$ both scale inversely proportional to the dataset size $|\mathcal{S}|$, meaning the larger the dataset the more reliable these estimators become. In the limit of infinitely many datapoints $|\mathcal{S}| \rightarrow \infty$, Eq. 5 peaks on $\mathcal{L}(w)$ and $\nabla \mathcal{L}(w)$. In the following sections in order to declutter notation, the position indicator (w) will be occasionally dropped, and $L_S(w)$ for example is replaced by L_S .

2.2. When to stop? An Evidence-Based Criterion

The estimators L_D and ∇L_D are approximately Gaussian distributed around \mathcal{L} and $\nabla \mathcal{L}$ respectively (Eq. 5). This means that in practice, by choosing a finite dataset of size $M := |\mathcal{D}|$ also *one* specific realization $[L_D, \nabla L_D]$ is chosen from this distribution. A different dataset of same size (but also drawn from $p(x)$) results in a different realization of $[L_D, \nabla L_D]$. This is illustrated in Figure 1 in a one-dimensional sketch. The left subplot shows the marginal distribution of function values (first line in Eq. 5). The true but usually unknown optimization objective \mathcal{L} (Eq. 1) is the mean of this distribution and is shown in solid orange. The objective L_D (Eq. 2), which is optimized in practice and is fixed by the training set \mathcal{D} , defines *one* realization out of this distribution and is shown in dashed blue.

In general, the minimizers of \mathcal{L} and L_D need not be the same. Often it is the case that for a finite but large number

of parameters $w \in \mathbb{R}^D$ the loss L_D can be optimized to be very small. When this is the case the model tends to overfits to the training data and thus performs poorly on newly generated (test) data $\mathcal{T} \sim p(x)$ with $\mathcal{T} \cap \mathcal{D} = \emptyset$. A widely used technique to prevent overfitting is to stop the optimization process early. The idea is that variations of training examples which do not contain information for generalization are mostly learned at the very end of the optimization process where the weights w are fine-tuned. In practice the true minimum of \mathcal{L} is unknown, however the approximate errors of the estimators L_D and ∇L_D are accessible at every position w . Local estimators for the diagonal of $\Sigma(w)$ have been successfully used before (Mahseeci & Hennig, 2015; Balles et al., 2016) and can be computed efficiently even for very high dimensional optimization problems. Here the variance estimator of the gradient distribution is denoted as $\hat{\Sigma}(w) \approx \mathbf{var}_{x \sim p(x)}[\nabla \ell(w, x)]$ with

$$\hat{\Sigma}(w) = \frac{1}{|\mathcal{S}| - 1} \sum_{x \in \mathcal{S}} (\nabla \ell(w, x) - \nabla L_S(w))^2 \quad (7)$$

where \cdot^2 denotes the elementwise product and \mathcal{S} is either the full dataset \mathcal{D} or a mini-batch \mathcal{B} .

Since the minimizers of \mathcal{L} and L_D are not generally identical, also their gradients will cross zero at different locations w . The middle plot of Figure 1 illustrates this behavior. Similar to the left plot, it shows a marginal distribution, but this time over gradients (second line in Eq. 5). The true gradient $\nabla \mathcal{L}$ is the mean of this distribution and is shown in solid orange. The *one* realization defined by the dataset \mathcal{D} is shown as dashed blue and corresponds to the dashed blue function values L_D of the left plot. Ideally the optimizer should stop in an area in w -space where possible minima are likely to occur, if different datasets of same size were samples from p . In the sketch this is encoded as red vertical shaded area in right plot of Figure 1. It is the area around the minimizer of \mathcal{L} where $\nabla \mathcal{L} \pm 1$ standard deviation still encloses zero.

Since $\nabla\mathcal{L}$ is unknown however this criterion is hard to use in practice. Let us denote the minimizer of \mathcal{L} as $w^* = \arg \min_w \mathcal{L}(w)$ and the population variance of gradients at w^* as $\Sigma^* := \Sigma(w^*)$. A similar criterion that captures this desiderata in essence is to stop when the collected gradients $\nabla L_{\mathcal{D}}$ are becoming consistently very small in comparison to the error $\frac{\Sigma^*}{M}$ (red horizontal shaded area). Close enough to the minima of $L_{\mathcal{D}}$ and \mathcal{L} , the two criteria roughly coincide (intersection of red vertical and horizontal shaded areas).

A measure for this is the marginal distribution $p(\nabla L_{\mathcal{D}})$, where $\nabla\mathcal{L}$ is integrated out. This is the probability that $\nabla L_{\mathcal{D}}$ would have if it was generated by a true zero gradient $\nabla\mathcal{L} = 0$. In other words the evidence of $\nabla L_{\mathcal{D}}$ under the assumption that $p(\nabla\mathcal{L}) = \delta(\nabla\mathcal{L})$ is

$$\begin{aligned} p(\nabla L_{\mathcal{D}}) &= \int p(\nabla L_{\mathcal{D}}|\nabla\mathcal{L}) p(\nabla\mathcal{L}) d\nabla\mathcal{L} \\ &= \mathcal{N}\left(\nabla L_{\mathcal{D}}; 0, \frac{\Sigma^*}{M}\right). \end{aligned} \quad (8)$$

If gradients $\nabla L_{\mathcal{D}}$ are becoming too small or, ‘too probable’ (stepping into the horizontal shaded area) the gradients are less likely to still carry information about $\nabla\mathcal{L}$ but rather represent noise due to the finiteness of the dataset, then the optimizer should stop. Using these assumptions, the next section derives a stopping criterion for the gradient decent algorithm which then can be extended to stochastic gradient descent as well.

2.3. Early Stopping Criterion for Gradient Descent

When using gradient descent, the whole dataset is used to compute the gradient $\nabla L_{\mathcal{D}}$ in each iteration (Eq. 3). Still this gradient estimator has an error in comparison to the true gradient $\nabla\mathcal{L}$, which is encoded in the covariance matrix Σ . In practice Σ is unknown, the variance estimator $\hat{\Sigma}$ described in Eq. 7 however is always accessible. In addition Eq. 8 requires the gradient variance Σ^* at the true minimum which is unknown in practice. Again it can be approximated by $\Sigma(w_t)$ which is the gradient variance at the current position of the optimizer w_t . This is a sensible choice if the optimizer is in convergence and already close to a minimum. Thus, at every position w an approximation to the evidence $p(\nabla L_{\mathcal{D}})$ of Eq. 8 is

$$p(\nabla L_{\mathcal{D}}(w)) \approx \prod_{k=1}^D \mathcal{N}\left(\nabla L_{\mathcal{D}}^k(w); 0, \frac{\hat{\Sigma}_k(w)}{M}\right). \quad (9)$$

Though being a simplification, this allows for fast and scalable computations since dimensions are treated independent of each other. To derive an early stopping criterion based only on $\nabla L_{\mathcal{D}}$ we borrow the idea of the previous section that the optimizer should halt when gradients become ‘too small’ in comparison to the information they still carry

about $\nabla\mathcal{L}$ and combine this with well known techniques from evidence-based hypothesis testing. Specifically stop when

$$\log p(\nabla L_{\mathcal{D}}) - \mathbf{E}_{\nabla L_{\mathcal{D}} \sim p}[\log p(\nabla L_{\mathcal{D}})] > \tilde{c} \quad (10)$$

for some constant \tilde{c} . Here $\mathbf{E}[\cdot]$ is the expectation operator. For $\tilde{c} = 0$ the optimizer stops when the logarithmic evidence of the gradients is larger than its expected value, roughly meaning that more gradient samples $\nabla L_{\mathcal{D}}$ lie inside of some expected range. In particular, combining Eq. 9 with Eq. 10 and scaling with the dimension D of the objective, gives

$$\begin{aligned} &\frac{2}{D} [\log p(\nabla L_{\mathcal{D}}) - \mathbf{E}_{\nabla L_{\mathcal{D}} \sim p}[\log p(\nabla L_{\mathcal{D}})]] \\ &= 1 - \frac{M}{D} \sum_{k=1}^D \left[\frac{(\nabla L_{\mathcal{D}}^k)^2}{\hat{\Sigma}_k} \right] > c \end{aligned} \quad (11)$$

with $c := 2 \cdot \tilde{c} / D$. This criterion is very intuitive, especially for $c = 0$. If all gradient elements lay at exactly one standard deviation distance to zero, then $\sum_k (\nabla L_{\mathcal{D}}^k)^2 / \hat{\Sigma}_k = \sum_k \hat{\Sigma}_k / M \cdot \hat{\Sigma}_k = D/M$. Thus the left hand side of Eq. 11 would become zero and the optimizer would stop.

We note on the side that Eq. 11 defines a mean criterion over all elements of the parameter vector w . This implicitly assumes that all dimensions converge in roughly the same time scale such that weighing the fractions $f_k := M \cdot (\nabla L_{\mathcal{D}}^k)^2 / \hat{\Sigma}_k$ equally is justified. If optimization problems deal with parameters that converge at different speeds, like for example different layers of neural networks (or biases and weights inside one layer) it might be appropriate to compute one stopping criterion per subset of parameters which are roughly having similar timescales. In Section 4.3 we will use this slight variation of Eq. 11 for experiments on a multi layer perceptron. Throughout all experiments of Section 4 we will use the most intuitive parameter of $c = 0$.

2.4. Stochastic Gradients and Mini-batching

It is straightforward to extend the stopping criterion derived in Eq. 11 to stochastic gradient descent (SGD). As described in Eq. 4 the estimator for $\nabla L_{\mathcal{D}}$ is replaced with an even more uncertain $\nabla L_{\mathcal{B}}$ by sub-sampling the training dataset at each iteration. The gradient generation according to Eq. 4 is

$$\begin{aligned} \nabla L_{\mathcal{D}} &= \nabla\mathcal{L} + \epsilon, \quad \epsilon \sim \mathcal{N}\left(0, \frac{\Sigma}{M}\right) \\ \nabla L_{\mathcal{B}} &= \nabla L_{\mathcal{D}} + \eta, \quad \eta \sim \mathcal{N}(0, \Sigma_{obs}) \\ &= \nabla\mathcal{L} + \nu, \quad \nu \sim \mathcal{N}\left(0, \frac{\Sigma}{M} + \Sigma_{obs}\right). \end{aligned} \quad (12)$$

Combining this with Eq. 5 yields $\Sigma/M + \Sigma_{obs} = \Sigma/m$. Thus $\Sigma_{obs} = \frac{M-m}{mM} \Sigma$. Equivalently to Eq. 8, 9 and 11, this results

in an early stopping criterion for stochastic gradient descent:

$$\begin{aligned} & \frac{2}{D} [\log p(\nabla L_{\mathcal{B}}) - \mathbf{E}_{\nabla L_{\mathcal{B}} \sim p} [\log p(\nabla L_{\mathcal{B}})]] \\ &= 1 - \frac{m}{D} \sum_{k=1}^D \left[\frac{(\nabla L_{\mathcal{B}}^k)^2}{\hat{\Sigma}_k} \right] > c. \end{aligned} \quad (13)$$

Again we will use $c = 0$ for all our experiments.

3. Implementation

Computing the stopping criterion is straight-forward, given that the variance estimate $\hat{\Sigma}(w)$ is available. In this case, it amounts to an element-wise division of the squared gradient by the variance, followed by an aggregation over all dimensions.

The variance estimate can be computed directly using Eq. (7) if the gradients $\ell(w, x)$ can be accessed individually for each example x . In many cases though, most notably in contemporary software frameworks for the training of neural networks, gradients are computed simultaneously and aggregated implicitly for efficiency. Balles et al. (2016, §4.2) comment on this issue and present a solution that computes the variance estimate implicitly, increasing the computational cost of a backward pass by a factor of about 1.25.

4. Experiments

For proof of concept experiments, we evaluate the stopping criterion derived in Section 2 on a number of standard classification and regression problems. Section 4.1 evaluates the stopping criterion on a least squares toy problem. Sections 4.2 and 4.3 deal with the more realistic setting of logistic regression on the well known breast cancer dataset¹ and a multi layer perceptron on the MNIST dataset² (LeCun et al., 1998).

4.1. Linear Least-Squares as Toy Problem

We begin with a toy regression problem on artificial data generated from a one-dimensional linear function y with additive uniform Gaussian noise. This simple setup allows us to illustrate the model fit at various stages of the optimization process and provides us with the true generalization performance, since we can generate large amounts of test data. We use a largely over-parametrized 50-dimensional linear regression model $\hat{y}(w, x) = w^T \phi(x)$ which contain the ground truth features (bias and linear) and additional periodic features with varying frequency. The features $\phi(x) = [1, x, \sin(a_1 x), \cos(a_1 x), \dots, \sin(a_p x), \cos(a_p x)]^T$ with

¹[http://archive.ics.uci.edu/ml/datasets/Breast+Cancer+Wisconsin+\(Diagnostic\)](http://archive.ics.uci.edu/ml/datasets/Breast+Cancer+Wisconsin+(Diagnostic))

²<http://yann.lecun.com/exdb/mnist/>

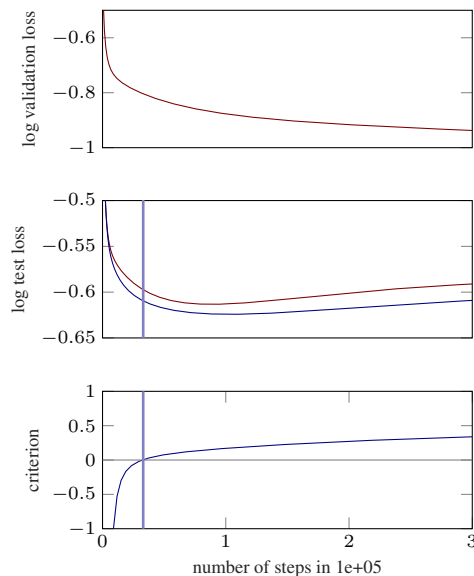


Figure 2. Results for *logistic regression* on the Wisconsin Breast Cancer dataset. Results for the two variants are color-coded; red for validation set-based early stopping, blue for the evidence-based criterion of Eq. 11. The **middle** plot shows test loss versus the number of optimization steps for both methods. The **top** row shows validation loss; since the validation loss decreases over the whole optimization process it does *not* induce a stopping point. The **bottom** row shows the evolution of the stopping criterion, inducing a stopping decision indicated by the blue vertical bar.

$p = 24$ obviously define a massively over-parametrized model for the true function and is thus prone to overfitting. We fit the model by minimizing the squared error, i.e. the loss function is $\ell(w, (x, y)) = \frac{1}{2}(y - \hat{y}(w, x))^2$. We use 20 samples for training and about 10 for validation, and then train the model using gradient descent. The results are shown in Figure 3. Both, validation loss, and the evidence-based stopping criterion find an acceptable point to stop the optimization procedure thus preventing overfitting.

4.2. Logistic Regression

Next, we apply the stopping criterion to logistic regression on the Wisconsin Breast Cancer dataset. The task is to classify cell nuclei (described by features such as radius, area, symmetry, et cetera) as either malignant or benign. We conduct a second-order polynomial expansion of the original 32 features (i.e., we add features of the form $x_i x_j$) resulting in 496 effective features used for the logistic regression. Of the 569 instances in the dataset, we withhold 369, a relatively large share, for testing purposes in order to get a reliable estimate of the generalization performance. The remaining 200 instances are available for training the classifier. We perform two training runs: one with early stopping based on a validation set of 60 instances (reducing the training

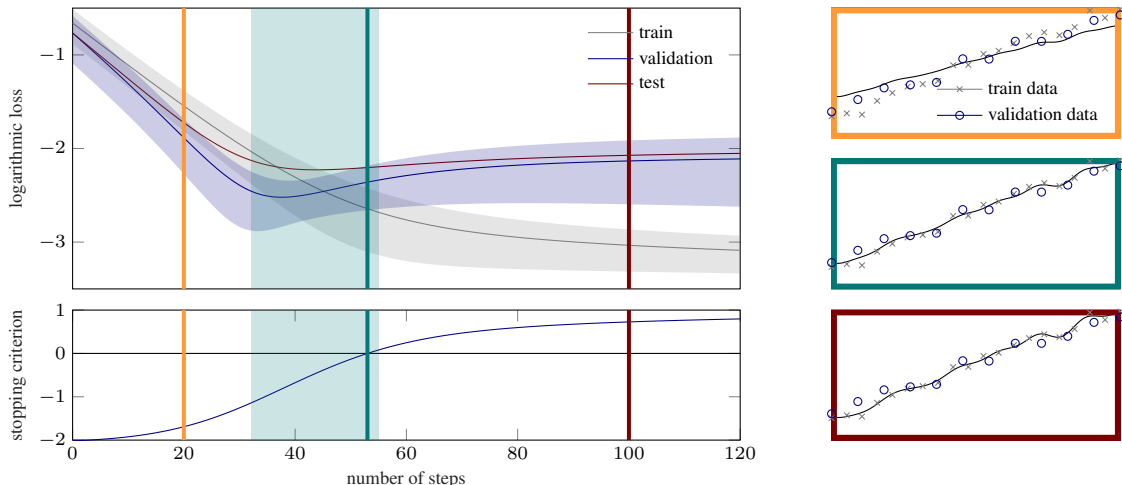


Figure 3. Results for the *least-squares toy problem*. The **top left** plot shows logarithmic losses over the number of optimization steps. The train loss (gray) decreases throughout the optimization process, whereas the ground-truth test loss (red) saturates after approximately 40 steps and increases thereafter. The validation loss (blue) is an uncertain estimate of the test loss; the shaded area indicates two standard deviations $\pm 2\sqrt{\Lambda/|S|}$ computed during the optimization (Eq. 5). Notice how the minimum of the validation loss is suboptimal in terms of the test loss, but falls into an acceptable region (green shaded area). The **bottom left** plot shows the evolution of the stopping criterion (Eq. 11) and the green vertical bar indicates the suggested stopping point; it is not exactly coinciding with the minimum of the true test loss, but falls into the acceptable region as well. For the steps marked with color-coded vertical bars, we illustrate the model fit on the **right-hand side**. At the orange iteration the training is still in progress as can be seen from the sub-optimal fit ($\hat{y}(w)$ in solid dark blue) to the training data (gray crosses). The green iteration shows the fit when the evidence-based stopping criterion of Eq. 11 indicates to halt. At the time of the red iteration the model \hat{y} has already overfitted to the training data.

set to 140 instances) and one using the full training set and early stopping with the evidence-based criterion derived in Section 2.3.

If parameters converge at different speeds during the optimization, as indicated in Section 2.3, it is sensible to compute the criterion separately for different subgroups of parameters. Generally, if we split the parameters into N disjoint subgroups $S_i \subset \{1, \dots, D\}$, and denote $D_i = |S_i|$, the criterion reads

$$\frac{1}{N} \sum_{i=1}^N \left(1 - \frac{M}{D_i} \sum_{k \in S_i} \left[\frac{(\nabla L_D^k)^2}{\hat{\Sigma}_k} \right] \right) > c. \quad (14)$$

Since bias and weight gradients usually have different magnitudes they converge at different speeds when trained with the same learning rate. For logistic regression, we thus treat the weight vector and the bias parameter of the logistic regressor as separate subgroups. Since the criterion of Eq 14 is noisy we also smooth it with an exponential running average.

The results are depicted in Figure 2. The effect of the additional training data is clearly visible, resulting in lower test losses throughout the optimization process. In this scarce data setting the validation loss, computed on a small set of only 60 instances, is clearly misleading (top plot in Fig. 2). It decreases throughout the optimization process and, thus,

fails to find a suitable stopping point. The bottom plot in Fig. 2 shows the evolution of our stopping criterion. The induced stopping point is not optimal (in that it does not coincide with the point of minimal test loss) but falls into an acceptable region. Thanks to the additional training data, the test loss at the stopping point is lower than any test loss attainable when withholding a validation set.

4.3. Multi-Layer Perceptron

Finally, we train a multi-layer perceptron (MLP) on the well-studied problem of hand-written digit classification on the MNIST dataset. The inputs to the net are 784-dimensional vectorized gray-scale images of handwritten digits. We use a MLP with five hidden layers with 2500, 2000, 1500, 1000 and 500 units, respectively, and ReLU activation. The output layer has 10 units (for the ten digit classes) with soft-max activation and we use standard cross-entropy loss. This architecture has approximately 12 million trainable parameters. We treat each weight matrix and each bias vector of the network as a separate subgroup in the sense of equation 14. The MNIST dataset contains 50k training images and a separate test set of 10k images. For comparison, we perform two training runs for each learning rate: one with early stopping based on a validation set of size 10k (consequently reducing the training set to 40k images) and one using the full training set and early stopping with the evidence-based

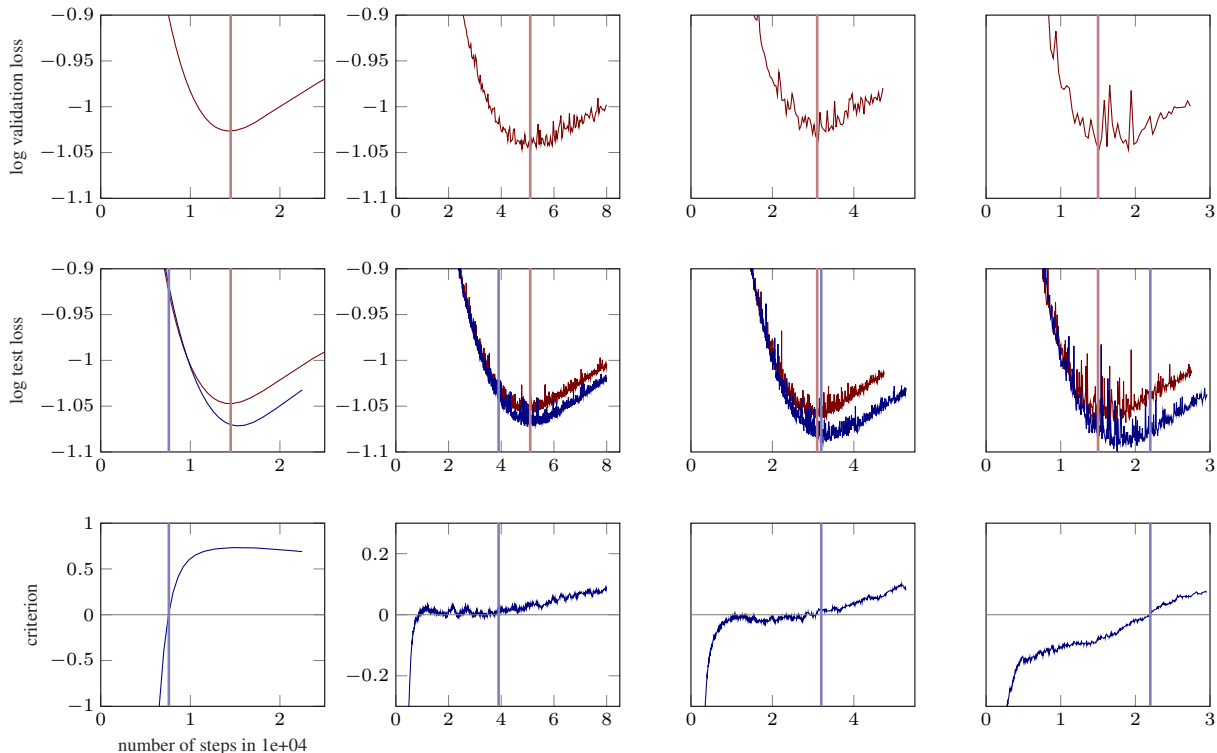


Figure 4. Results for *multi-layer perceptron* on MNIST. The columns correspond to different training configurations. The **leftmost column** is gradient descent with a learning rate of 0.01. **Columns 2-4** show results for SGD with a mini-batch size of 128 and learning rates 0.003, 0.005 and 0.01, respectively. Results for the two variants are color-coded; red for validation set-based early stopping, blue for the evidence-based stopping criterion. The **middle row** shows logarithmic test loss versus the number of optimization steps for both methods. The **top row** shows logarithmic validation loss; the point of minimal validation loss induces a stopping decision indicated by the red vertical bar. The bottom row shows the evolution of the evidence-based stopping criterion, inducing a stopping decision indicated by the blue vertical bar. Since for MNIST the validation loss is a very good estimator for the generalization loss it very reliably induces good stopping points. Against this strong competitor the evidence-based stopping criterion performs as good as or better for the SGD-runs and slightly worse for the gradient descent run.

stopping criterion. Again the criterion is smoothed by an exponential running average.

The results are shown in Figure 4. The relatively large validation set (10k images) yields accurate estimates of the generalization performance. Consequently, the stopping points more or less coincide with the points of minimal test loss. The reduced training set size leads to only slightly higher test losses. Since the strength of the evidence-based criterion is to utilize the additional training data and the fact, that also validation losses are only inexact guesses of the generalization error, both of these points thus favor the early stopping criterion based on the validation loss. Still for all three SGD-runs (columns 2-4 in Figure 4) the evidence-based criterion performs as good as or better than the validation set induced method. An additional observation is that, the quality of the stopping points induced by the evidence-based method varies between the different training configurations. It is thus arguably not as stable in comparison to setups where the validation loss is *very* reliable.

For gradient descent (full training set in each iteration) our method however (an very similarly to the gradient descent runs on the logistic regression problem) chooses to stop a bit too early, and thus does result in a slightly worse test set performance. The difference is not very much (note the zoomed in ordinate ranging form $10^{-1.1}$ to $10^{-0.9}$) but it also clearly does not outperform the nearly exactly positioned stopping point induced by this well calibrated validation loss.

4.3.1. GREEDY ELEMENT-WISE STOPPING

For the early stopping criterion (Eq. 11), we compute $f_k = m(\nabla L_B^k)^2 / \hat{\Sigma}_k$ for each gradient element k . This quantity can be understood as a ‘signal-to-noise ratio’. For the stopping decision, the individual f_k are aggregated (over the whole parameter vector or over subgroups of parameters) and the training is stopped when the *mean* falls below a threshold. As a side experiment, we employ the same idea in an element-wise fashion: we stop the training for an individual parameter $w_k \in \mathbb{R}$ (not to be confused with the full

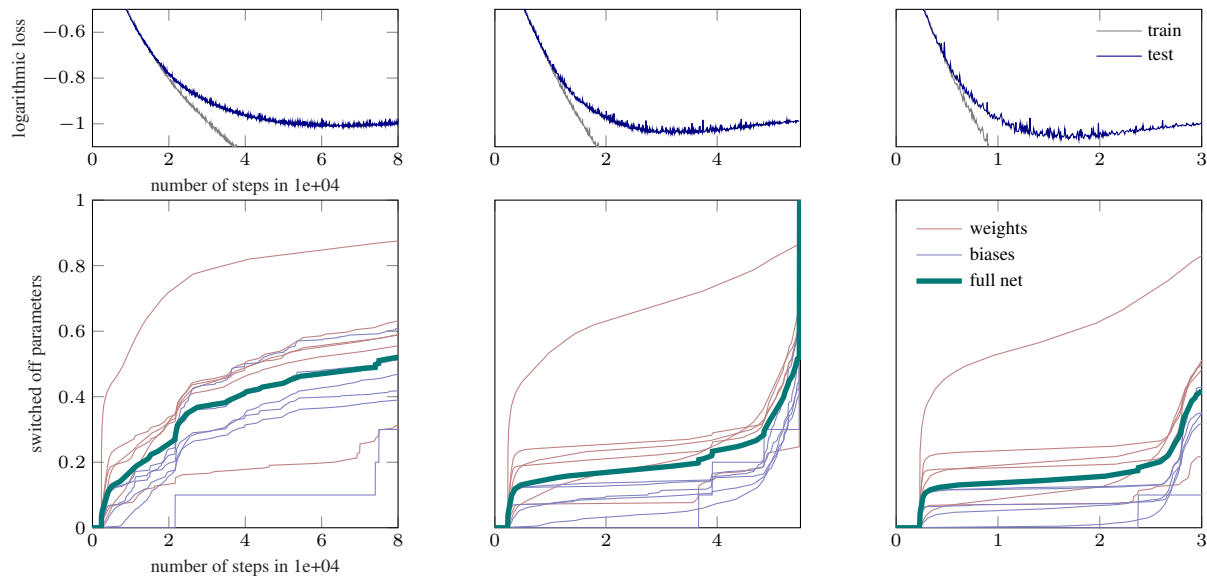


Figure 5. Results for *greedy element-wise stopping* for a multi-layer perceptron on MNIST. The **columns** correspond to different training configurations, showing results for SGD with a batch size of 128 and learning rates 0.003, 0.005 and 0.01, respectively. The **top row** shows logarithmic training and test loss. The **bottom row** shows the fraction of weights that have been halted by the greedy element-wise stopping, individually for each weight matrix (red) and each bias vector (blue), as well as for the full network (green).

parameter vector $w_t \in \mathbb{R}^D$ at iteration t) as soon as f_k falls below the threshold. Importantly this is *not* a sparsification of the parameter vector, since w_k is not set to zero when being switched off, but merely fixed at its current value. Since the individual f_k are quite noisy, we smooth them over multiple steps using an exponential moving average; this was not necessary in the aggregate criterion, where variations in the f_k average out. The moving averages are initialized at high values, resulting in a warm-up phase where all weights are ‘active’.

Figure 5 presents results. Intriguingly, immediately after the warm-up phase the training of a considerable fraction of all weights (10 percent or more, depending on the training configuration) is being stopped. This fraction increases further as training progresses. Especially towards the end where overfitting sets in, a clear signal can be seen; the fraction of weights where learning has been stopped suddenly increases at a higher rate. Despite this reduction in effective model complexity, the network reaches test losses comparable to our training runs without greedy element-wise stopping (compare to the test losses in Fig. 4). The fraction of switched-off parameters towards the end of the optimization process reaches up to 80 percent in a single layer and around 50 percent for the whole net.

5. Conclusion

We presented a novel approach to the problem of determining a good point for early-stopping in gradient-based

optimization. In contrast to existing methods it does not rely on a held-out validation set and enables the optimizer to utilize all available training data.

Instead, we exploit fast-to-compute statistics of the observed gradient to assess when it represents noise originating from the finiteness of the training set, instead of an informative gradient direction. To do this, we estimate the evidence of the evaluated gradients under the assumption that the gradient of the true underlying function is zero.

The presented method so far is applicable in gradient descent as well as stochastic gradient descent settings and adds little overhead in computation, time, and memory consumption. The assumptions made are reasonable for most machine learning settings, so that the method is widely applicable.

In our experiments, we presented results for linear least-squares fitting, logistic regression and a multi-layer perceptron, proving the general concept to be viable. Furthermore, preliminary findings on element-wise early stopping open up the possibility to monitor and control model fitting with a higher level of detail.

References

- Balles, Lukas, Romero, Javier, and Hennig, Philipp. Coupling Adaptive Batch Sizes with Learning Rates. *ArXiv e-prints*, December 2016.
- Bishop, Christopher M. *Pattern Recognition and Machine Learning*. Springer, 2006.

- Goodfellow, Ian, Bengio, Yoshua, and Courville, Aaron. *Deep Learning*. MIT Press, 2016.
- He, Kaiming, Zhang, Xiangyu, Ren, Shaoqing, and Sun, Jian. Deep residual learning for image recognition. In *Proceedings of the IEEE Conference on Computer Vision and Pattern Recognition (CVPR)*, pp. 770–778, 2016.
- Krizhevsky, Alex, Sutskever, Ilya, and Hinton, Geoffrey E. Imagenet classification with deep convolutional neural networks. In *Advances in Neural Information Processing Systems (NIPS)*, volume 25, pp. 1097–1105, 2012.
- Krogh, Anders and Hertz, John A. A simple weight decay can improve generalization. In *Advances in Neural Information Processing Systems (NIPS)*, volume 4, pp. 950–957, 1991.
- LeCun, Yann, Bottou, Léon, Bengio, Yoshua, and Haffner, Patrick. Gradient-based learning applied to document recognition. *Proceedings of the IEEE*, 86(11):2278–2324, 1998.
- Maclaurin, Dougal, Duvenaud, David, and Adams, Ryan P. Early stopping is nonparametric variational inference. Technical Report arXiv:1504.01344 [stat.ML], 2015.
- Mahsereci, Maren and Hennig, Philipp. Probabilistic line searches for stochastic optimization. In *Advances in Neural Information Processing Systems (NIPS)*, volume 28, pp. 181–189, 2015.
- Morgan, Nelson and Bourlard, Hervé. Generalization and parameter estimation in feedforward nets: Some experiments. In *Proceedings of the 2nd International Conference on Neural Information Processing Systems*, pp. 630–637. MIT Press, 1989.
- Prechelt, Lutz. *Early Stopping — But When?*, pp. 53–67. Springer Berlin Heidelberg, Berlin, Heidelberg, 2012. ISBN 978-3-642-35289-8. doi: 10.1007/978-3-642-35289-8_5.
- Reed, Russell. Pruning algorithms—a survey. *IEEE transactions on Neural Networks*, 4(5):740–747, 1993.
- Sietsma, Jocelyn and Dow, Robert JF. Creating artificial neural networks that generalize. *Neural networks*, 4(1): 67–79, 1991.
- Simonyan, Karen and Zisserman, Andrew. Very deep convolutional networks for large-scale image recognition”. *CoRR*, abs/1409.1556, 2014.
- Szegedy, Christian, Liu, Wei, Jia, Yangqing, Sermanet, Pierre, Reed, Scott, Anguelov, Dragomir, Erhan, Dumitru, Vanhoucke, Vincent, and Rabinovich, Andrew. Going deeper with convolutions. In *Proceedings of the IEEE Conference on Computer Vision and Pattern Recognition (CVPR)*, 2015.
- Tibshirani, Robert. Regression shrinkage and selection via the lasso. *Journal of the Royal Statistical Society. Series B (Methodological)*, pp. 267–288, 1996.
- Vincent, Pascal, Larochelle, Hugo, Bengio, Yoshua, and Manzagol, Pierre-Antoine. Extracting and composing robust features with denoising autoencoders. In *Proceedings of the 25th International Conference on Machine Learning (ICML)*, pp. 1096–1103. ACM, 2008.